# Defect annihilation and morphological improvement of hydrothermally grown ZnO nanorods by Ga doping

A. Escobedo-Morales and U. Pal

Citation: Applied Physics Letters **93**, 193120 (2008); doi: 10.1063/1.3026746
View online: http://dx.doi.org/10.1063/1.3026746
View Table of Contents: http://scitation.aip.org/content/aip/journal/apl/93/19?ver=pdfcov
Published by the AIP Publishing

# Defect annihilation and morphological improvement of hydrothermally grown ZnO nanorods by Ga doping

A. Escobedo-Morales and U. Pal[a)]
*Instituto de Física, Universidad Autónoma de Puebla, Apdo. Postal J-48, Puebla, Pue 72570, Mexico*

(Received 2 August 2008; accepted 24 October 2008; published online 14 November 2008)

One dimensional zinc oxide nanostructures were grown by a low temperature hydrothermal process. Effects of Ga doping on the growth, crystallization, and defect distribution in them were studied by x-ray diffraction, scanning electron microscopy, photoluminescence, and Fourier-transform infrared spectroscopy techniques. It has been shown that Ga doping improves the morphological homogeneity and optical properties of ZnO nanostructures. Improved morphology of the doped nanostructures have been associated with the catalytic effect of Ga. Effects of Ga doping on the quenching of defect emission and improvement of excitonic emission in ZnO nanostructures are discussed. © *2008 American Institute of Physics*. [DOI: 10.1063/1.3026746]

Zinc oxide (ZnO) is one of the most attractive semiconductors with wide band gap (3.37 eV at room temperature) and high exciton binding energy (60 meV), promising for optical and electronic applications.[1–3] In nanostructure form, it has received even wider applications such as light emitting diodes,[4] lasers,[5] field emission devices,[6] phosphors,[2] chemical sensors,[7] and catalysts[8] to mention a few. As the properties and hence applications of ZnO nanostructures depend strongly on their size, shape, defect concentration, or doping, along with surface characteristics, varieties of its morphologies including nanowires,[5] nanorods,[9] nanorings,[10] and nanohelices[10] are reported. Several physical[5,11,12] and chemical[13,14] techniques have been developed to fabricate ZnO nanostructures with well defined shapes and sizes.

In the present letter, we describe the synthesis of one dimensional (1D) Ga doped ZnO structures of nanometer/submicrometer diameters through a low temperature hydrothermal process and their optical properties. Ga doping modifies drastically the morphology and electronic defect structures of ZnO nanostructures, making them more suitable for optoelectronic applications.

The following chemicals were purchased commercially and used as received without further purification: ethylenediamine [EDA, $NH_2(CH_2)_2NH_2$; Baker, 99.9%], zinc acetate dihydrate [$Zn(CH_3COO)_2 \cdot 2H_2O$; Aldrich, 99.99%], sodium hydroxide (NaOH; Aldrich, 99.99%), and gallium (III) nitrate hydrate [$Ga(NO)_3 \cdot xH_2O$; Aldrich, 99.999%]. In a three neck round bottom flask, 108 ml of de-ionized water (18.0 MΩ cm) and 12 ml of EDA were mixed under vigorous stirring. To the previous alkaline solution, 10.25 g of zinc acetate was added. After further addition of 1.70 g of anhydrous NaOH, the *p*H of the solution turned to 12. The flask containing the solution was then heated at 110 °C for 15 h in an oil bath. After cooling, the product was extracted by decantation, washed several times with de-ionized water, and dried in a muffle furnace. To obtain the doped samples, measured amounts of gallium nitrate were added to the alkaline solution before heating. Nominal 0.5%, 1.0%, and 2.0% Ga doped samples were synthesized, adding 0.060, 0.119, or 0.239 g of gallium salt (nominal Ga mol % $= \mathrm{Ga}[M]/\mathrm{Zn}[M] \times 100\%$).

Structure, morphology, and elemental composition of the samples were studied using x-ray diffraction (XRD) (Phillips X'Pert diffractometer with Cu $K\alpha$ radiation), scanning electron microscopy (SEM) (Jeol JSM 5300), and energy dispersive x-ray spectroscopy (EDS) (Thermo Noran SuperDry II) techniques. Influence of gallium doping on the optical properties of the samples was studied by room temperature photoluminescence (PL) using the 325 nm line of a He–Cd laser and Fourier-transform infrared (FTIR) (Nicolet Magna 750) spectroscopies. The acquired PL spectra of the samples were corrected using the spectral responses of the monochromator and detector (photomultiplier).

SEM micrographs of undoped ZnO sample [Fig. 1(a)] revealed a flowerlike morphology composed of needlelike structures of about 300 nm diameter and several micrometer length. On gallium doping, the diameter of the needlelike crystals increased noticeably. Although the flowerlike or forestlike arrangement of the 1D structures remained even on 2.0% Ga doping, their needlelike morphology changed to nail-like structures with uniform diameter and well defined tips [Fig. 1(d) and inset therein].

XRD patterns of doped and undoped ZnO structures [Fig. 1(e)] revealed well defined diffraction peaks related to ZnO in wurtzite phase,[15] with no additional peak related either to Ga or its oxides. While the well defined XRD peaks of similar intensities and widths (Table I) indicate similar crystallinity of the doped and undoped samples, no appreciable shift in peak positions indicate the absence of lattice distortion due to Ga doping. Since Zn and Ga have similar atomic radii (1.38 and 1.41 Å, respectively), no considerable distortion of ZnO lattice is expected by gallium doping.

Although a betterment of crystallinity and morphological modification in ZnO nanostructures on Ga doping was observed by Liang *et al.*[16] for their 1D ZnO nanostructures in vapor growth process and was correlated with the catalytic effect of Ga, they could not detect the presence of Ga in their ZnO nanostructures. In contrast, the presence of Ga and their increased content with the increase of nominal doping concentration in our samples were confirmed by EDS (Table I).

Room temperature PL spectra of the doped and undoped samples (Fig. 2) revealed two emissions: an UV emission

a)Author to whom correspondence should be addressed. FAX: +52–222–2295611. Electronic mail: upal@sirio.ifuap.buap.mx.

 

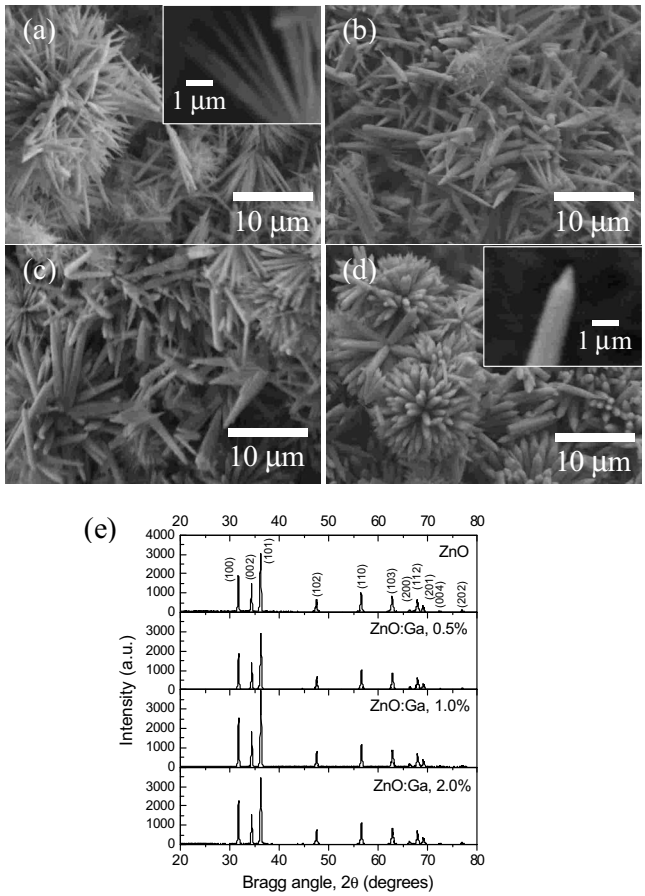


FIG. 1. Typical SEM micrographs of (a) undoped, (b) 0.5%, (c) 1.0%, and (d) 2.0% Ga doped samples and (e) corresponding XRD patterns.

centered at about 3.2 eV and a broad visible emission located at around 2.1 eV. The intensity of the UV emission, which is related to free exciton (FX) recombination in ZnO,[17–20] increased and broadened considerably with the increase of gallium doping. The position of the FX band maximum (~3.23 eV for undoped sample) also suffered a redshift on Ga doping (Table I). Incorporation of shallow levels below the conduction band due to Ga doping could be responsible for the redshift of FX emission and its broadening.

Unlike the FX emission, the broad visible emission is quenched with gallium doping. On deconvolution of the visible emission, there appeared six subbands denoted as infrared (~1.61 eV), red (~1.75 eV), orange (~1.95 eV), yellow (~2.20 eV), green (~2.40 eV), and blue (~2.60 eV), with predominant yellow and orange emissions. The observed infrared emission at about 1.61 eV

TABLE I. Elemental composition, FWHM of main XRD peak, and estimated band gap of doped and undoped ZnO samples. The energy band gap ($E_g$) was estimated by adding the FX binding energy ($E_b$=60 meV) to the observed FX emission energy ($E_g$=FX+$E_b$).

| Nominal Ga doping (mol %) | Zn:O:Ga, at. % EDS (average)[a] | (101) FWHM (deg) | $E_g$ (eV) PL (FX+60 meV) |
|---|---|---|---|
| 0.0 | 50:50:0 | 0.23 | 3.291 ± 0.003 |
| 0.5 | 49.63:50.08:0.29 | 0.23 | 3.279 ± 0.003 |
| 1.0 | 49.44:50.11:0.45 | 0.22 | 3.285 ± 0.003 |
| 2.0 | 48.73:50.26:1.02 | 0.22 | 3.274 ± 0.003 |

[a]Error of EDS measurements: ±0.05 at. %.

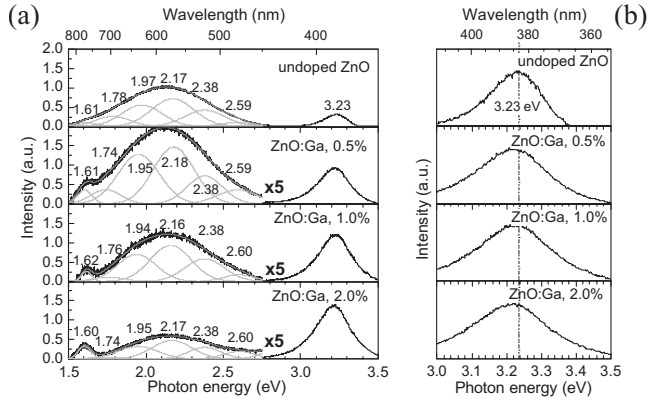


FIG. 2. (a) Room temperature PL spectra of the doped and undoped ZnO nanostructures and (b) corresponding free excitonic emissions after intensity normalization.

corresponds to the first harmonic of FX emission. While green emission is by far the most common visible emission observed in ZnO grown by physical techniques such as thermal evaporation,[17,18] yellow or orange emissions are commonly observed in hydrothermally grown ZnO.[14] Oxygen deficiencies ($V_O$) are widely accepted as the origin of green emission in ZnO.[20–22] Recently Jannoti *et al.*[23] attributed this emission to the electronic transitions associated with zinc vacancies ($V_{Zn}$). As the yellow and orange emissions frequently appear together, it is feasible that they have common defect origins. Nevertheless, their origins remain uncertain. Interstitial zinc ($Zn_i$) and singly ionized interstitial oxygen ($O_i^-$) were proposed[20–22] as their origins. It is believed that $Zn_i$ and $V_O$ are the common defects in ZnO,[24,25] which are responsible for *n*-type conductivity and green emission in ZnO, respectively. Nevertheless in O-rich samples like that synthesized by hydrothermal methods, $O_i$ is the predominant defect, which is a deep acceptor level. The studies of Janotti *et al.*[23] indicate that in O-rich *n*-type ZnO, $V_{Zn}$ and $O_i$ are by far the predominant defects, which can explain the yellow and orange emissions observed in our samples. Origins of red and blue emissions are still more controversial and unclear. However, they are believed to be associated with the shallow $V_O$ and $Zn_i$ levels, respectively.[19,26]

Figure 3 shows the evolution of FX band and defect emission intensities with respect to the nominal concentra-

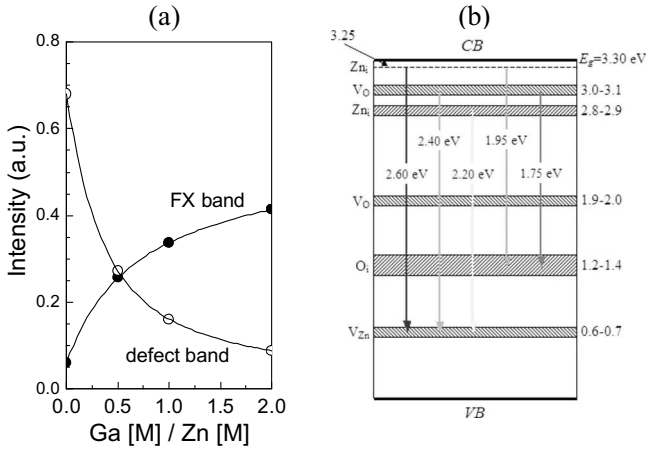


FIG. 3. (a) Intensity variation in the FX emission and defect related broad band as a function of nominal doping concentration. (b) Proposed schematic energy band diagram for the ZnO samples. Energies of defect bands are given with respect to the top of the valence band in eV.

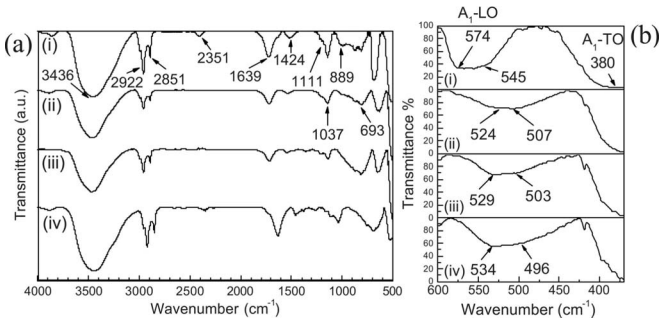


FIG. 4. (a) FTIR spectra of (i) undoped and (ii) 0.5%, (iii) 1.0%, and (iv) 2.0% Ga doped ZnO nanostructures. (b) The amplified 370–600 $cm^{-1}$ region of the corresponding samples.

tion of gallium doping. While the FX emission increases with Ga content exponentially, the intensity of defect emission decays exponentially, demonstrating clearly the native defect quenching in ZnO nano-/submicrostructures or generation of nonradiative defect centers due to Ga doping.

Figure 4(a) shows the FTIR spectra of the doped and undoped samples. All the spectra are similar in the range of 600–4000 $cm^{-1}$. The bands located at 3436 and 1639 $cm^{-1}$ are attributed to stretching and bending modes of the hydroxyl (–OH) group of water molecules adsorbed on ZnO surfaces.[27] Traces of EDA used in the reaction remained adsorbed in the samples. The bands located at 2922 and 2851 $cm^{-1}$ correspond to stretching modes,[28] and the bands centered at 1424 $cm^{-1}$ correspond to the bending mode of $–CH_2$ groups.[28] While the band centered at about 1037 $cm^{-1}$ is the stretching mode of the carbon chain in EDA,[28] the band located around 889 $cm^{-1}$ is related to the WAG mode of amine ($–NH_2$) group.[28] The bands at about 2351 and 693 $cm^{-1}$ correspond to stretching and bending modes of atmospheric carbon dioxide adsorbed on the ZnO surface, respectively.[27]

In the 370–600 $cm^{-1}$ spectral range [Fig. 4(b)], the undoped sample revealed two bands at around 380 and 560 $cm^{-1}$. While the 380 $cm^{-1}$ band is attributed to the $A_1$-TO mode of wurtzite ZnO, the asymmetric nature of the second band suggests that it is composed of at least two subbands. The components are discernible clearly at about 574 and 545 $cm^{-1}$, which correspond to $A_1$-LO and $B_2$-high modes of ZnO, respectively.[8] In doped samples, the position of the $A_1$-TO mode remained almost fixed. However, the superimposed LO and $B_2$-high modes moved toward lower frequencies by about 50 $cm^{-1}$. Formation of local vibrational modes (LVMs) due to $Ga_{Zn}$ sites is not responsible for such redshifts as the Ga atoms are heavier than Zn atoms. Furthermore, the LVMs formed by gallium doping are expected at higher frequencies. It is well known that the LO modes are sensitive to the dielectric constant of the material. Zn and Ga are the elements of groups IIB and IIIB, respectively. If Ga atoms are incorporated as substitutional, each Ga atom adds an extra charge carrier to the ZnO lattice. Increase in the charge carrier density also results in the modification of dielectric constant. Therefore, it is feasible that the frequency of the LO mode could be shifted by gallium doping toward lower frequencies.[29] It is worth noting that the LO band gets broader and intense with the increase of gallium doping. We believe that this band is indeed composed of the $B_2$-high silent mode and LO mode, which were activated and shifted toward lower frequencies due to modification of dielectric constant on gallium doping.

In conclusion, it has been shown that the Ga doping improves the morphological homogeneity and annihilates defect content in hydrothermally grown ZnO nanostructures. Although due to similar atomic radii of Zn and Ga the incorporation of Ga in ZnO lattice does not create additional lattice defects, the extra charge incorporated by Ga doping modifies the frequency of the $A_1$-LO mode and activate $B_2$-high mode, which is generally silent in FTIR spectra of ZnO.

The authors are thankful to Dr. M. Herrera Zaldívar and E. Aparacio for their help in taking SEM images and XRD spectra. The work was partially supported by VIEP-BUAP, Mexico.

[1] Z. W. Pan, Z. R. Dai, and Z. L. Wang, Science **291**, 1947 (2001).
[2] C. H. Lin, B. S. Chiou, C. H. Chang, and J. D. Lin, Mater. Chem. Phys. **77**, 647 (2003).
[3] A. Kashyout, M. Soliman, K. El Gamal, and M. Fathy, Mater. Chem. Phys. **90**, 230 (2005).
[4] S. Y. Lee, E. S. Shim, H. S. Kang, S. S. Pang, and J. S. Kang, Thin Solid Films **473**, 31 (2005).
[5] M. H. Huang, S. Mao, H. Feick, H. Yan, Y. Hu, H. Kind, E. Weber, R. Russo, and P. Yang, Science **292**, 1897 (2001).
[6] Y. W. Zhu, H. Z. Zhang, X. C. Sun, S. Q. Feng, J. Xu, Q. Zhao, B. Xiang, R. M. Wang, and D. P. Yu, Appl. Phys. Lett. **83**, 144 (2003).
[7] Z. Fan and J. G. Lu, Appl. Phys. Lett. **86**, 123510 (2005).
[8] Ü. Özgür, Y. I. Alivov, C. Liu, A. Teke, M. A. Reshchikov, S. Dogan, V. Avrutin, S. J. Cho, and H. Morkoc, J. Appl. Phys. **98**, 041301 (2005).
[9] P. X. Gao, D. Yong, and Z. L. Wang, Nano Lett. **3**, 1315 (2003).
[10] X. Y. Kong and Z. L. Wang, Nano Lett. **3**, 1625 (2003).
[11] Y. C. Kong, D. P. Yu, B. Zhang, W. Fang, and S. Q. Feng, Appl. Phys. Lett. **78**, 407 (2001).
[12] A. B. Hartanto, X. Ning, Y. Nakata, and T. Okada, Appl. Phys. A: Mater. Sci. Process. **78**, 299 (2004).
[13] W. I. Park, Y. H. Jun, S. W. Jung, and G. C. Yi, Appl. Phys. Lett. **82**, 964 (2003).
[14] U. Pal and P. Santiago, J. Phys. Chem. B **109**, 15317 (2005).
[15] JCPDS Card No. 36–1451.
[16] Y. Liang, X. Zhang, L. Qin, E. Zhang, H. Gao, and Z. Zhang, J. Phys. Chem. B **110**, 21593 (2006).
[17] B. D. Yao, Y. F. Chan, and N. Wang, Appl. Phys. Lett. **81**, 757 (2002).
[18] X. Zhang, Y. Zhang, J. Xu, Z. Wang, X. Chen, D. Yu, P. Zhang, H. Qi, and Y. Tian, Appl. Phys. Lett. **87**, 123111 (2005).
[19] X. Q. Wei, B. Y. Man, M. Liu, C. S. Xue, H. Z. Zhuang, and C. Yang, Physica B **388**, 145 (2007).
[20] X. L. Wu, G. G. Siu, C. L. Fu, and H. C. Ong, Appl. Phys. Lett. **78**, 2285 (2001).
[21] E. De la Rosa, S. Sepúlveda-Guzman, B. Reeja-Jayan, A. Torres, P. Salas, N. Elizondo, and J. M. Yacaman, J. Phys. Chem. C **111**, 8489 (2007).
[22] A. B. Djurisic, Y. H. Leung, K. H. Tam, L. Ding, W. K. Ge, H. Y. Chen, and S. Gwo, Appl. Phys. Lett. **88**, 103107 (2006).
[23] A. Janotti and C. G. Van de Walle, Phys. Rev. B **76**, 165202 (2007).
[24] A. A. Sokol, S. A. French, S. T. Bromley, R. A. Catlow, H. J. J. van Dam, and P. Sherwoode, Faraday Discuss. **134**, 267 (2007).
[25] S. B. Zhang, S.-H. Wei, and A. Zunger, Phys. Rev. B **63**, 075205 (2001).
[26] J. H. Cai, G. Ni, G. He, and Z. Y. Wu, Phys. Lett. A **372**, 4104 (2008).
[27] N. B. Colthup, L. H. Saly, and S. E. Wiberly, *Introduction to Infrared and Raman Spectroscopy*, 3rd ed. (Academic, New York, 1990).
[28] M. G. Giorgini, M. Rosaria, G. Paliani, and R. S. Caraliotti, J. Raman Spectrosc. **14**, 16 (1983).
[29] H. Fujiwara and M. Kondo, Phys. Rev. B **71**, 075109 (2005).